

# Electric quadrupole effects and nuclear spin relaxation in a $\text{Al}_{72.4}\text{Pd}_{20.5}\text{Mn}_{7.1}$ icosahedral quasicrystal studied by NMR

T. Apih, O. Plyushch,\* M. Klanjšek, and J. Dolinšek  
*J. Stefan Institute, Jamova 39, SI-1000 Ljubljana, Slovenia*

(Received 1 June 1999)

The  $^{27}\text{Al}$  NMR spectrum and the spin-lattice relaxation rate of an icosahedral  $\text{Al}_{72.4}\text{Pd}_{20.5}\text{Mn}_{7.1}$  quasicrystal were studied in the temperature range from 300 to 4 K at two magnetic fields. The results are compatible with the hypothesis that a screening electron cloud is formed around the Mn ions in an aluminum-rich environment, which together with the core electrons produces a large electric-field gradient (EFG) at the sites of the Al nuclei. The EFG is temperature dependent due to the polarization of the screening cloud and the core electrons by the magnetic moments of the Mn unpaired  $d$  electrons. The shift of the  $^{27}\text{Al}$  central line shows an inverse magnetic-field dependence and appears to be of an electric quadrupolar origin. The  $^{27}\text{Al}$  spin-lattice relaxation rate shows an  $aT + bT^3$  temperature dependence that can be explained by approximating the quasicrystalline electronic structure by a two-band model, consisting of a broad  $s$  and a narrow  $d$  conduction bands. The  $T^3$  term originates from the narrowness of the  $d$  band. The  $^{27}\text{Al}$  spin-lattice relaxation in  $\text{Al}_{72.4}\text{Pd}_{20.5}\text{Mn}_{7.1}$  is governed by two relaxation mechanisms of similar strength, the electric quadrupole and the magnetic hyperfine. The quadrupole mechanism is stronger at high temperatures such as room temperature whereas the magnetic relaxation dominates at low temperatures. [S0163-1829(99)02746-0]

## I. INTRODUCTION

Quasicrystals (QC) are solid materials exhibiting a new type of a perfect long-range order without translational periodicity. Their symmetries (icosahedral, dodecagonal, decagonal, octagonal, and pentagonal) involve “forbidden” symmetry elements such as fivefold rotation axes that are incompatible with the periodicity of a Bravais lattice. A consequence of nonperiodicity is that phonons and electrons cannot propagate easily through the lattice so that QC’s—being alloys of metallic elements—exhibit transport phenomena that resemble more insulating than metallic character. Structurally highly ordered QC’s are characterized by a very high electrical resistivity and semi-insulating behavior, showing a proximity of a metal-to-insulator transition at low temperature.<sup>1–6</sup> It was conjectured that the low electrical conductivity results from the formation of a pseudogap in the electronic density of states (DOS) at the Fermi energy<sup>7,8</sup> that was shown to be a generic property of QC’s and their approximants.<sup>9</sup> The existence of the pseudogap plays an essential role in the stability of QC structures as the minimum in the DOS at the Fermi level stabilizes the structure by a significant reduction of the total electronic energy.<sup>8</sup> Band-structure calculations for icosahedral QC structures predicted that narrow peaks and valleys of the DOS should be present inside the broad pseudogap. Such sharp features were experimentally reported in an NMR relaxation study<sup>10</sup> but there still remains some controversy on their existence.<sup>11,12</sup>

In ordinary metals, the electronic DOS at the Fermi level  $g(E_F)$  can be conveniently studied by nuclear magnetic resonance (NMR). In the presence of conduction electrons the shift of the nuclear resonance frequency  $K = (\nu - \nu_0)/\nu_0$  due to electronic hyperfine magnetic fields (the Knight shift) is proportional to  $g(E_F)$ , whereas the spin-lattice relaxation rate shows a quadratic dependence on the DOS;  $1/T_1$

$\propto [g(E_F)]^2$ . NMR studies of quasicrystals mostly assume a predominantly metallic character of these substances and—despite the evident difference from ordinary metals—analyze the data in the frame of the simple metal NMR theory. Several spin-lattice relaxation studies performed on QC samples assumed a magnetic relaxation<sup>10,11,13,14</sup> due to  $s$ -type conduction electrons as dominant. An unusual temperature dependence of the relaxation rate of the type  $T_1^{-1} = aT + bT^\alpha$  with  $\alpha \approx 2-3$  was interpreted as a sign of sharp features in the pseudogap.<sup>10,13</sup> The generalization of the metallic relaxation to QC’s due to the  $s$  conduction electrons is, however, not straightforward. QC’s are poor electrical conductors with a low DOS at the Fermi level. In addition, strong parallel relaxation mechanisms may exist, such as electric quadrupole relaxation via the fluctuating electronic and ionic charges, core polarization effects and the relaxation via paramagnetic centers (such as localized  $\text{Mn}^{2+}$   $d$ -electron moments in Mn-containing QC’s) in combination with spin diffusion.

In this paper we present a  $^{27}\text{Al}$  NMR spectrum, Knight shift and spin-lattice relaxation study of an icosahedral  $\text{Al}_{72.4}\text{Pd}_{20.5}\text{Mn}_{7.1}$  single-grain quasicrystal that contains a small number of magnetic Mn ions. We show that the assumption of a dominant magnetic relaxation due to the  $s$ -type conduction electrons is too restrictive and cannot account even qualitatively for the observed magnetic-field dependence of the  $^{27}\text{Al}$  relaxation rate. The total relaxation rate contains several relaxation contributions of magnetic and electric quadrupole origin of similar strength that are not easy to resolve. Comparison of the relaxation and the Knight shift data indicates the existence of a strong—if not the dominant—quadrupolar relaxation mechanism in  $\text{Al}_{72.4}\text{Pd}_{20.5}\text{Mn}_{7.1}$ . We also show that the magnetic and electric quadrupolar relaxation mechanisms via the conduction electrons both result in relaxation rates of the form  $aT + bT^3$ . This form can be derived generally for a two-band

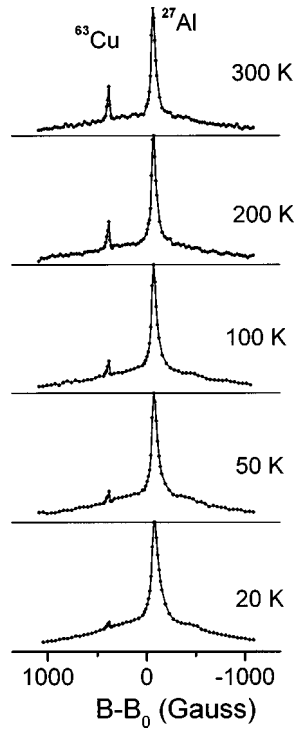


FIG. 1.  $^{27}\text{Al}$  field-swept NMR spectra of a single-grain icosahedral quasicrystal  $\text{Al}_{72.4}\text{Pd}_{20.5}\text{Mn}_{7.1}$  ( $B_0 = 2.35$  T,  $\nu_0(^{27}\text{Al}) = 26.134$  MHz, five-axis oriented perpendicular to  $B_0$ ). The  $^{63}\text{Cu}$  line originates from the probehead coil. The spectra are scaled to equal height.

metal, where a broad  $s$  and a narrow  $d$  electron bands coexist. The reason for the appearance of the  $T^3$  term is the narrowness of the  $d$  band and the presence of this term by itself does not prove the existence of sharp features inside the pseudogap.

## II. $^{27}\text{Al}$ NMR LINE SHAPE AND FREQUENCY SHIFT

The  $^{27}\text{Al}$  NMR experiment was performed on an icosahedral  $\text{Al}_{72.4}\text{Pd}_{20.5}\text{Mn}_{7.1}$  single-grain crystal grown by the Czochralsky technique and further annealed at  $800^\circ\text{C}$ . The crystal was oriented in the magnetic field with the five-axis perpendicular to  $B_0$ . The spectra were obtained by a magnetic field-sweep technique where the spin-echo intensity was recorded as a function of the field strength. The  $^{27}\text{Al}$  ( $I = \frac{5}{2}$ ) spectra measured in the temperature interval 300–20 K at  $\nu_0(^{27}\text{Al}) = 26.134$  MHz (corresponding to the center absorption field of 2.35 T) are displayed in Fig. 1. The strongly inhomogeneously broadened spectrum shows a typical structure of a broad ‘‘background’’ line, representing first-order quadrupole-perturbed satellite transitions, and a narrow central line, quadrupole-perturbed in second order.<sup>15</sup> The central lines of the spectra in Fig. 1 exhibit a continuous broadening on cooling that increases approximately as  $1/T$  [Fig. 2(a)].

A similar temperature dependence was observed also in the measurement of the shift  $\Delta\nu = \nu - \nu_0$  of the  $^{27}\text{Al}$  central line position [Fig. 2(b)]. The shift was measured with respect to the aqueous solution of  $\text{AlCl}_3$ . A metallic Al powder sample was measured for calibration and its Knight shift was found to be positive (paramagnetic), amounting to  $K$

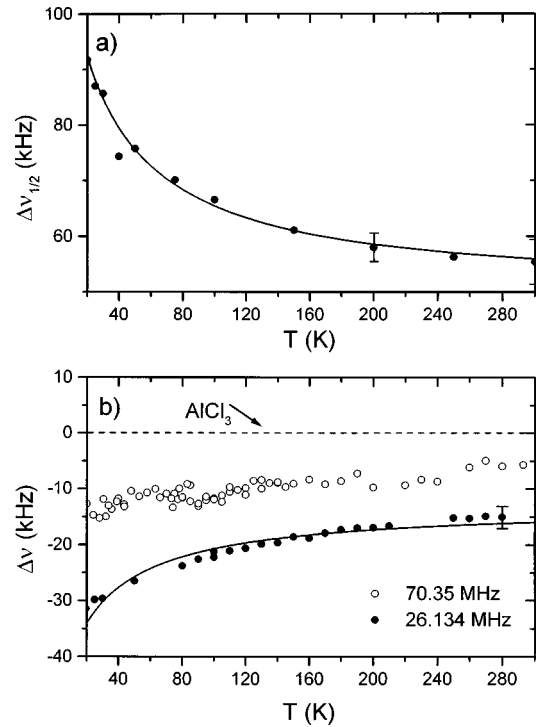


FIG. 2. Temperature dependence of (a) the full width at half height  $\Delta\nu_{1/2}$  and (b) the frequency shift  $\Delta\nu = \nu - \nu_0$  of the  $^{27}\text{Al}$  NMR central line in  $\text{Al}_{72.4}\text{Pd}_{20.5}\text{Mn}_{7.1}$  at two magnetic fields 2.35 and 6.3 T (with the respective  $^{27}\text{Al}$  resonance frequencies of 26.134 and 70.35 MHz). The shifts are measured relative to the  $\text{AlCl}_3$  aqueous solution. Solid lines represent the fits described in the text.

$= \Delta\nu/\nu_0 = 1.8 \times 10^{-3}$ . In contrast, the  $^{27}\text{Al}$  shift of  $\text{Al}_{72.4}\text{Pd}_{20.5}\text{Mn}_{7.1}$  was found negative and an order of magnitude smaller, amounting to  $-1.9 \times 10^{-4}$  at room temperature. On cooling  $K$  follows the same inverse temperature dependence as the central linewidth and reaches the value  $-6.3 \times 10^{-4}$  at 20 K. The measurement of the shift was repeated in a three times higher field of 6.3 T and  $\Delta\nu$  was found to be reduced to one third of its low-field value, meanwhile exhibiting the same temperature dependence. The shift has thus decreased in higher field and not increased linearly with the field as expected for the Knight shift in the usual sense, originating from the local magnetic fields of conduction electrons. The inverse field dependence of the shift  $\Delta\nu \propto 1/H$  supports the conclusion that the observed shift represents the second-order electric quadrupolar shift.

The temperature dependence of the  $^{27}\text{Al}$  central line broadening and frequency shift in the studied temperature range 300–20 K can be explained by the influence of the magnetic Mn ions on the conduction and core electrons that determine the electric field gradient (EFG) at the  $^{27}\text{Al}$  sites. It is known that in structurally perfect icosahedral Al-Pd-Mn QC's a small amount of Mn sites (typically about 1%) is magnetic<sup>16,17</sup> and can carry a large  $d$ -electron magnetic moment up to several  $\mu_B$ . Such paramagnetic centers act in a way as paramagnetic impurities in a metallic matrix. Friedel<sup>18</sup> has shown in a pioneering work on transition-metal impurities in simple metals that an impurity, because of its different valency, acts as a scattering potential to the conduction electrons. The consequence of scattering is a buildup (or depletion) of electronic charge around the impurity that

screens out the excess nuclear charge, leaving the system locally charge neutral. The screening produces a long-range oscillating charge density—known as Friedel oscillations—that far away from the impurity has a form<sup>19</sup>  $\rho(r) \propto (1/r^3)\cos 2k_F r$ . Here  $k_F$  is the Fermi wave vector and  $r$  has the origin at the impurity. The charge-density oscillations result in an oscillating electric field gradient (EFG) that still has to be corrected for antishielding by the core electrons of the host metal atoms at the position of their nuclei.<sup>19,20</sup> Assuming that the impurities produce an axially symmetric EFG, the oscillating gradient  $q$  can be written in the form<sup>21</sup>

$$q = (2\alpha/\pi r^3)\mu \cos(2k_F r + \varphi), \quad (1)$$

where  $\alpha$  and  $\varphi$  are determined by the scattering center and  $\mu$  is an enhancement factor due to the core polarization. In diluted Al-Mn alloys<sup>20</sup>  $\mu$  was found to be about 15.

In Mn-containing QC's, such as the Al-Pd-Mn family, a Friedel oscillationslike screening electron cloud around the Mn ions, situated in an aluminum-rich environment, can exist as well. The icosahedral phase in this system forms in a relatively narrow range around the ideal icosahedral composition  $\text{Al}_{70}\text{Pd}_{22}\text{Mn}_8$ , so that the environment of any Mn or Pd atom is in principle aluminum rich. In addition, only a fraction of about 1% of all Mn ions are magnetic, so that these paramagnetic centers can be considered as diluted. This resembles analogy to the diluted Al-Mn alloys where the concept of Friedel oscillations is well established.<sup>21</sup>

The screening cloud together with the Al core electrons produces a large EFG at the <sup>27</sup>Al nuclear sites. The presence of  $d$  moments at magnetic Mn sites, that couple via the exchange interaction to the screening and core electrons, further influences the electronic EFG via the polarization of the electron cloud and makes it temperature dependent. This coupling increases the gradient in proportion to the thermal-average value of the  $d$ -electron spin  $\langle S_d \rangle$  that depends on temperature according to the Curie-Weiss law as  $1/(T-\theta)$  (or  $1/T$ , provided the correlations between  $d$  electrons can be neglected). Since several magnetic Mn ions affect the EFG at a particular <sup>27</sup>Al site and these paramagnetic centers are distributed randomly in space, the temperature dependence of the EFG tensor may be predicted only qualitatively to follow approximately an inverse temperature dependence;  $q \propto 1/T$ . The second-order quadrupolar frequency shift  $\Delta\nu$  and the central linewidth  $\Delta\nu_{1/2}$  are both proportional to  $q^2/H$  and should thus depend on temperature as  $1/T^2$  in this approximation. Experimental <sup>27</sup>Al frequency shift and linewidth in  $\text{Al}_{72.4}\text{Pd}_{20.5}\text{Mn}_{7.1}$  [Figs. 2(a) and 2(b)], however, do not follow exactly neither the  $1/T$  nor the  $1/T^2$  dependence, but something in between. Good fits [solid lines in Figs. 2(a) and 2(b)] could be made by assuming the fit functions in the form  $\Delta\nu_{1/2} = a + b/(T-\theta)$  and  $\Delta\nu = c + d/(T-\theta)$  with  $a = 50$  kHz,  $b = 1950$  kHz K,  $c = -13$  kHz,  $d = -965$  kHz K and  $\theta = -26$  K, but due to a large number of fit parameters these fits should be considered as qualitative only.

### III. <sup>27</sup>Al SPIN-LATTICE RELAXATION

The <sup>27</sup>Al line shape and shift demonstrate the dominance of the electric quadrupole interaction over the magnetic hyperfine coupling in  $\text{Al}_{72.4}\text{Pd}_{20.5}\text{Mn}_{7.1}$ . However, conduction

electrons are present in this sample too and should have an observable effect on the NMR spin-lattice relaxation rate. In particular, the existence of a magnetic hyperfine interaction between the nuclear magnetic moments and the moments of conduction electrons should yield a strong—if not the dominant—magnetic relaxation mechanism even in the presence of a large electric quadrupolar interaction.

The <sup>27</sup>Al spin-lattice relaxation rate  $T_1^{-1}$  was measured in the temperature interval between 300 and 4 K at two different magnetic fields 2.35 and 6.3 T (corresponding to the <sup>27</sup>Al resonance frequencies of 26.134 and 70.35 MHz, respectively). The rates were determined on the <sup>27</sup>Al central line from the magnetization recovery following a saturation train of 60  $\pi/2$  pulses, separated by 30  $\mu\text{s}$ . In view of the possible quadrupolar effects, the magnetization-recovery curves were analyzed independently with the models of magnetic and electric quadrupole relaxation.

For magnetic relaxation<sup>22</sup> the magnetization recovery is described by a single relaxation rate  $T_1^{-1}$ :

$$M(t) = M_0 \{ 1 - [a_1 \exp(-t/T_1) + a_2 \exp(-6t/T_1) + a_3 \exp(-15t/T_1)] \}. \quad (2)$$

For short saturation (only  $\pm \frac{1}{2}$  levels are disturbed), the coefficients  $a_i$  amount to  $a_1 = 0.02857$ ,  $a_2 = 0.17778$ , and  $a_3 = 0.7936$  whereas for long saturation (again only  $\pm \frac{1}{2}$  levels are disturbed by the rf field, but the other levels can adjust their populations to establish a quasiequilibrium with the irradiated levels) the coefficients are  $a_1 = 0.25714$ ,  $a_2 = 0.26667$ , and  $a_3 = 0.47617$ .

In the case of quadrupolar relaxation there exist two relaxation rate constants  $W_1$  and  $W_2$  that are the  $\Delta m = \pm 1$  and  $\Delta m = \pm 2$  nuclear spin transition probabilities. The two rates can be extracted from the magnetization-recovery curves following the standard quadrupolar relaxation analysis<sup>23</sup> for spin  $I = \frac{5}{2}$ .

The <sup>27</sup>Al magnetization-recovery curves at temperatures 200 and 40 K are displayed in Figs. 3(a) and 3(b) together with the fits. The model of magnetic relaxation following short saturation yields an unsatisfactory fit to the experimental data, whereas the models of long-saturation magnetic relaxation and quadrupolar relaxation both yield excellent fits that reproduce the data points to practically equal precision. This is demonstrated in Fig. 3(c) where the mean square deviations  $\chi^2$  of the fits are compared for all three models. The quadrupolar fit actually yields the smallest  $\chi^2$  in the whole measured temperature range whereas the long-saturation magnetic fit yields an only insignificantly larger  $\chi^2$ . The  $M(t)$  curves alone thus cannot be used as a criterion to discriminate between the magnetic and quadrupolar relaxation mechanisms.

The <sup>27</sup>Al  $T_1^{-1}$ , determined from the long-saturation magnetic relaxation model, is displayed in Fig. 4(a). The rate was determined at two magnetic fields of 2.35 and 6.3 T and the data show quite a strong dependence on the magnetic field. The temperature dependence of  $T_1^{-1}$  was analyzed with two different fitting functions. The first Ansatz assumed a sum of a linear and a cubic term in the form

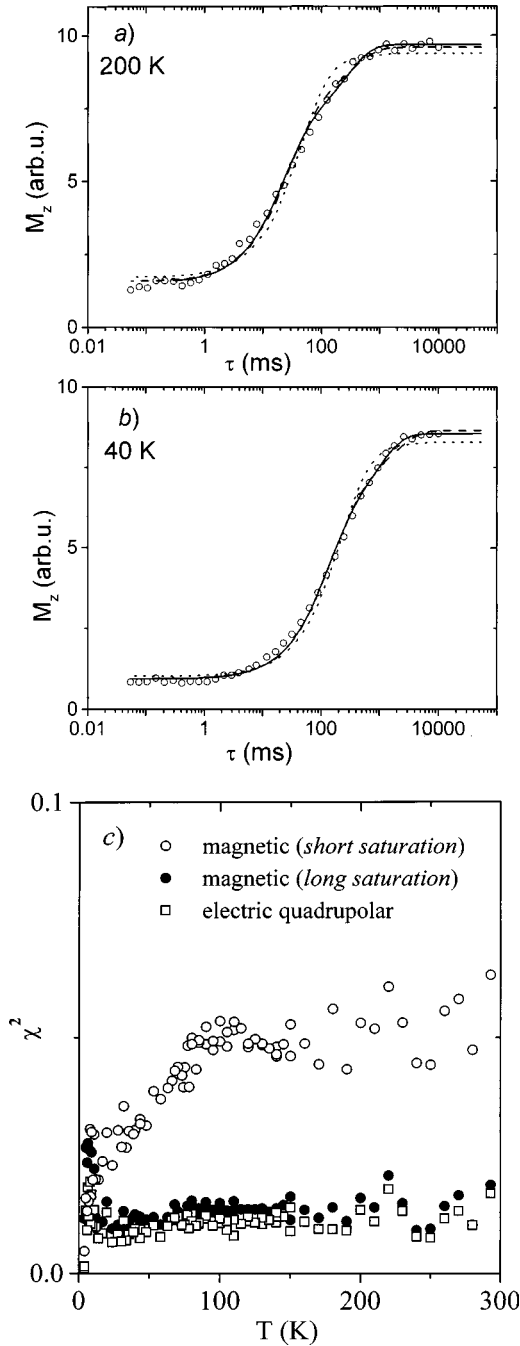


FIG. 3.  $^{27}\text{Al}$  nuclear spin magnetization-recovery curves following a saturation train of rf pulses in  $\text{Al}_{72.4}\text{Pd}_{20.5}\text{Mn}_{7.1}$  at (a) 200 K and (b) 40 K. Each set of data is fitted with three theoretical functions, corresponding to the short- (dotted line) and long-saturation (dashed line) magnetic relaxation conditions and to the electric quadrupolar relaxation model (solid line). Note that the dashed and the solid lines can be distinguished only at long delay times. In (c) the mean square deviations  $\chi^2$  of all three fits are shown in the whole measured temperature interval.

$$\frac{1}{T_1} = aT + bT^3. \quad (3)$$

As will be discussed later, this form can be derived analytically for a two-band metal, where a broad  $s$  and a narrow  $d$  conduction bands coexist. The second Ansatz does not have

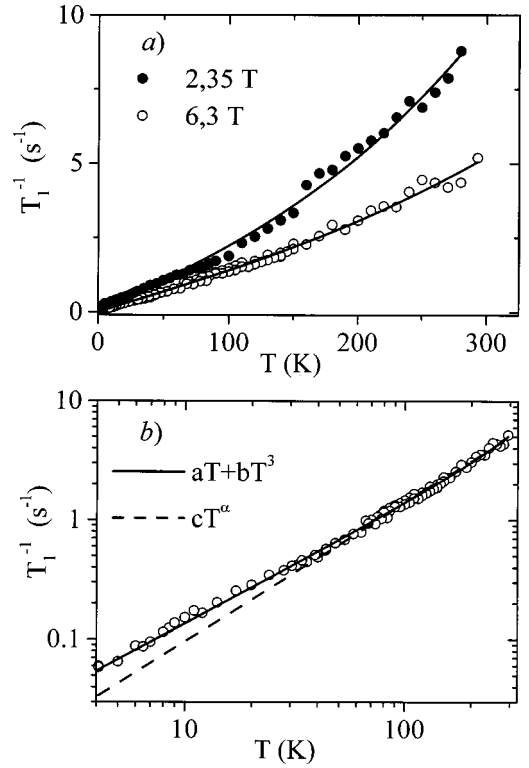


FIG. 4. (a)  $^{27}\text{Al}$  spin-lattice relaxation rate  $T_1^{-1}$  as a function of temperature, determined from the magnetization-recovery curves using the long-saturation magnetic relaxation model. The rate was determined at two magnetic fields of 2.35 (solid circles) and 6.3 T (open circles). Solid lines are fits with  $T_1^{-1} = aT + bT^3$ . (b) the 6.3-T data from (a) displayed in the log-log scale, showing comparison between the fits  $T_1^{-1} = aT + bT^3$  (solid line) and the power-law function  $T_1^{-1} = cT^\alpha$  (dashed line).

much physical background and was taken as a power-law form

$$\frac{1}{T_1} = cT^\alpha. \quad (4)$$

This form was used for comparison with Eq. (3) in order to get an insight on the uniqueness and reliability of the fit procedure.

An excellent fit to the data was obtained with Eq. (3) [solid lines in Fig. 4(a)]. The linear coefficient was found to be independent of the magnetic field and amounted to  $a = (1.7 \pm 0.3) \times 10^{-2} \text{ s}^{-1} \text{ K}^{-1}$  whereas the cubic term showed a pronounced field dependence and amounted to  $b = 1.27 \times 10^{-7} \text{ s}^{-1} \text{ K}^{-3}$  for the field 2.35 T and  $b = 4.28 \times 10^{-8} \text{ s}^{-1} \text{ K}^{-3}$  for 6.3 T. The total relaxation rate is thus smaller in a higher field. The simple power-law fit of Eq. (4), on the other hand, did not yield a satisfactory fit. In Fig. 4(b) both fits are compared on a log-log scale for the 6.3 T data. It is observed that Eq. (3) fits the data well in the whole temperature range whereas the power-law fit reproduces the data well only within a limited temperature range 300–30 K with  $\alpha = 1.16$ . At lower temperatures the experimental points deviate systematically from the  $\alpha$  fit. The above analysis demonstrates that Eq. (3) yields a reliable fit to the experimental data.

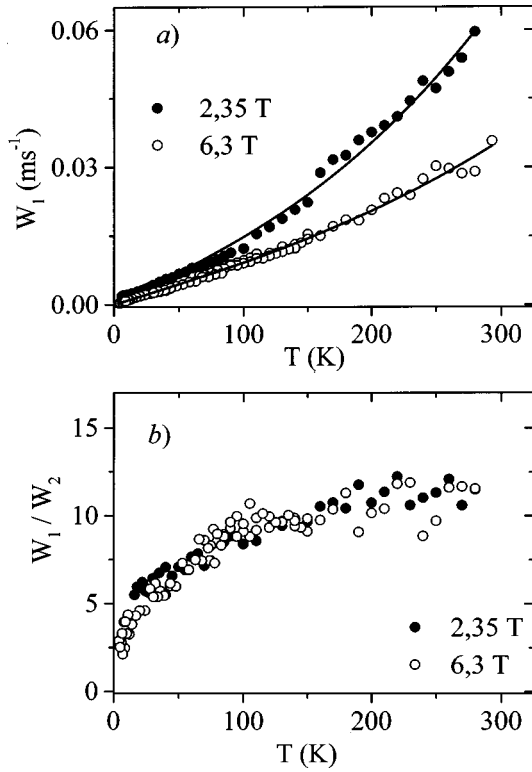


FIG. 5. (a)  $^{27}\text{Al}$  quadrupolar spin-lattice relaxation rate  $W_1$  and (b) the ratio  $W_1/W_2$  as a function of temperature and magnetic field (solid circles: 2.35 T, open circles: 6.3 T). The quadrupolar rates  $W_1$  and  $W_2$  were determined by the quadrupolar relaxation model from the same magnetization-recovery data as the magnetic rate  $T_1^{-1}$  shown in Fig. 4(a). Solid lines are fits with  $W_1 = aT + bT^3$ .

The same  $^{27}\text{Al}$  relaxation data were reanalyzed also with the model of electric quadrupole relaxation, yielding the two quadrupolar relaxation rates  $W_1$  and  $W_2$ . In Fig. 5 the rate  $W_1$  and the ratio  $W_1/W_2$  are shown as a function of temperature and magnetic field.  $W_1$  exhibits practically identical temperature and field dependence as the magnetic relaxation rate  $T_1^{-1}$ , displayed in Fig. 4(a). The temperature dependence could again be best reproduced by the sum of a linear and a cubic term;  $W_1 = aT + bT^3$  [solid line in Fig. 5(a)]. The linear coefficient was again found field independent;  $a = (1.15 \pm 0.25) \times 10^{-4} \text{ s}^{-1} \text{ K}^{-1}$ ; whereas the cubic term showed a significant field dependence and amounted to  $b = 9.5 \times 10^{-10} \text{ s}^{-1} \text{ K}^{-3}$  for the field of 2.35 T and  $b = 3.4 \times 10^{-10} \text{ s}^{-1} \text{ K}^{-3}$  for 6.3 T. The ratio  $W_1/W_2$  is approximately constant in the temperature interval 300–100 K and amounts to a factor of about 10, demonstrating a rather large difference between the  $W_1$  and  $W_2$  transition rates. Below 100 K, however, the ratio is getting smaller and approaches the value  $W_1/W_2 \approx 1$  at 4 K. This demonstrates that at lower temperatures the relaxation is governed increasingly more by a single relaxation rate constant. Since there is no special reason why  $W_1$  and  $W_2$  should become equal at low temperatures, this result very likely demonstrates the crossover from a dominant electric quadrupole relaxation (described by two relaxation rates) at high temperature to a dominant magnetic relaxation (described by a single  $T_1^{-1}$ ) at low temperature. The  $^{27}\text{Al}$  spin-lattice relaxation thus appears to be gov-

erned by two competing relaxation mechanisms—magnetic and electric quadrupolar—of similar strengths.

#### IV. DISCUSSION

In a theoretical description of the spin-lattice relaxation in the Al-Pd-Mn quasicrystals one encounters the problem of how to treat the conduction electrons as well as the unpaired  $d$  electrons of the magnetic Mn ions. In the absence of specific models that give a proper description of electron behavior in QC's it is tempting to use available theories, i.e., those which apply to either periodic crystals or amorphous alloys. In metals with a periodic lattice, conduction electrons are treated as extended waves in the form of plane or Bloch waves whereas in amorphous alloys the electron states are localized on the atomic scale. In QC's, on the other hand, the electrons are neither extended nor localized but occupy "critical" states<sup>24</sup> that are localized on a scale over many interatomic distances. To calculate the spin-lattice relaxation rate in the presence of such electrons is a difficult task at present due to a lack of a proper theoretical description of critical states. One is thus forced to perform an approximate analysis with the existing relaxation models. The most suitable model for the Al-Pd-Mn QC family turns out to be that of a two-band metal where the conduction electrons form a broad  $s$  and a narrow  $d$  band. In the Al-Pd-Mn system there exist two kinds of  $d$  electrons, those of Pd and Mn.

In a two-band metal the electrons (assumed to be noninteracting) occupy the  $s$  and  $d$  bands, having, respectively, the density of states at the Fermi level  $g_s(E_F)$  and  $g_d(E_F)$ . The  $s$ -state density  $g_s(E_F)$  is assumed to be constant over the energy interval  $k_B T$  around  $E_F$  whereas the  $d$ -state density  $g_d(E_F)$  varies appreciably over that interval due to the narrowness of the  $d$  band. Its behavior in the vicinity of  $E_F$  can be described by<sup>25</sup>

$$g_d(E) \approx g_d(E_F) + (E - E_F)g'_d(E_F) + \frac{1}{2}(E - E_F)^2 g''_d(E_F), \quad (5)$$

where  $g'_d(E_F)$  and  $g''_d(E_F)$  are first and second derivatives of  $g_d$  at the Fermi level. In addition, the narrowness of the  $d$  band implies that the Fermi energy itself becomes a function of temperature<sup>25</sup>

$$E_F = E_F^0 - \frac{\pi^2}{6} (k_B T)^2 \frac{g'_d(E_F^0)}{g_d(E_F^0)}. \quad (6)$$

Here  $E_F^0$  is the Fermi energy at  $T = 0$ .

In calculating the relaxation rate for a two-band metal, several magnetic contributions of comparable magnitude are found.<sup>25</sup> The  $s$ -band electrons give a contribution due to the contact interaction

$$(T_1^{-1})_s \propto k_B T [g_s(E_F)]^2. \quad (7)$$

The  $d$ -band electrons give the dominant contributions due to the orbital interaction and the core-polarization effect. Both contributions exhibit the same temperature dependence that can be calculated from

$$(T_1^{-1})_d \propto \int_0^\infty n(E)[1-n(E)][g_d(E)]^2 dE. \quad (8)$$

Here  $n(E) = \{\exp[(E-E_F)/k_B T] + 1\}^{-1}$  is the Fermi-Dirac function. Taking into account the narrowness of the  $d$  band given by Eqs. (5) and (6), one obtains the temperature dependence of the  $d$ -electron relaxation rate as

$$(T_1^{-1})_d \propto k_B T [g_d(E_F^0)]^2 \left\{ 1 + \frac{\pi^2}{3} (k_B T)^2 \frac{g_d''(E_F^0)}{g_d(E_F^0)} \right\} \quad (9)$$

that contains a linear and a cubic-in- $T$  term. The origin of the  $T^3$  term is thus the narrowness of the  $d$  band, or more precisely the fact that the variation of  $g_d(E)$  is not small over  $k_B T$  around  $E_F$ . The sum of the two magnetic contributions  $T_1^{-1} = (T_1^{-1})_s + (T_1^{-1})_d$  then leads to Eq. (3). Here it should be noted that a temperature dependence of the type of Eq. (9) (with  $g_d$  being replaced by  $g_s$ ) can be derived also for Korringa relaxation through the  $s$ -band electrons only,<sup>13</sup> provided one lifts the assumption that  $g_s$  is constant over the energy interval  $k_B T$  around  $E_F$ , but instead varies with the energy according to Eq. (5). In a two-band metal this Korringa  $s$ -band  $T^3$  correction should be small as compared to the  $T^3 d$ -band term, due to the broadness of the  $s$  band with respect to the  $d$  band.

In addition to the above magnetic contributions, conduction electrons provide also an electric quadrupolar contribution to the total relaxation rate. In ordinary metals the quadrupolar contribution is usually small compared to the magnetic one and is therefore neglected. The  $^{27}\text{Al}$  line shape and shift in  $\text{Al}_{72.4}\text{Pd}_{20.5}\text{Mn}_{7.1}$ , however, demonstrate the presence of strong electric quadrupole interaction in this quasicrystal so that the quadrupolar term can contribute significantly also to the spin-lattice relaxation. The quadrupolar spin transition probabilities  $W_1$  and  $W_2$  due to the conduction electrons were calculated by Obata.<sup>26</sup> For a two-band metal one finds the temperature-dependent part of each of the rates  $W_i$  to be given again by Eqs. (7) and (9) for the  $s$  and  $d$  electrons, respectively, thus yielding again to  $W_i = aT + bT^3$ .

There still remains a puzzling question as to why the  $^{27}\text{Al}$  spin-lattice relaxation rates exhibit a pronounced magnetic-field dependence. In simple metals the relaxation rates of electronic origin (either magnetic or electric quadrupolar) show no field dependence. In the electron-nucleus relaxation process the total electronic energies involved are of the order of  $E_F$  (that is typically of several eV) whereas the respective electronic and nuclear Zeeman energies are of the order of  $10^{-4}$  and  $10^{-7}$  eV. The Zeeman energies can be neglected in the total-energy balance of the nuclear spin relaxation process via conduction electrons, thus yielding field-independent relaxation rates. The above discrepancy between the theory and experiment may indicate that the two-band metal model is not fully adequate for application to quasicrystals. In view of the difference between the extended and critical states it is easy to anticipate this failure of the simple-metal theory in QC's, but difficult to correct at present due to the lack of a proper description of the critical states.

Another possible explanation of the field dependence of the relaxation rates is the existence of ionic contribution to the total quadrupolar relaxation rate. Localized vibrations of

atomic clusters (about 1 nm in length scale), which are excited at high temperature, were reported previously<sup>27</sup> in icosahedral  $\text{Al}_{65}\text{Cu}_{20}\text{Fe}_{15}$ . Such localized vibrational modes time modulate the EFG and can cause efficient spin-lattice relaxation, provided the fluctuation frequencies have a spectral component at the nuclear Larmor frequency ( $\sim 10^8$  Hz). This ionic contribution can be further enhanced by the Sternheimer antishielding effect due to the ionic electric-field polarization of the core electrons. The quadrupolar contribution from slow ionic fluctuations with frequencies smaller than the Larmor frequency would result in a relaxation rate inversely proportional to the square of the magnetic field, yielding larger relaxation rate in a smaller field. This consideration is in qualitative agreement with the experimental  $^{27}\text{Al}$  relaxation rates at high temperatures where at, e.g., 300 K the rate measured at 2.35 T is a factor of 2 larger from that at 6.3 T. Further work is, however, needed to clarify this point.

The fact that the field dependence appears increasingly smaller on going towards lower temperatures may be attributed to the same effect as the decrease  $W_1/W_2 \rightarrow 1$ , thus to the fact that on lowering the temperature the field-independent magnetic relaxation contribution starts to dominate over the quadrupolar mechanism. The observed decreasing field dependence of the rates as well as the decreasing difference between  $W_1$  and  $W_2$  on cooling thus appear artificially and do not represent real changes of the quadrupolar relaxation parameters.

## V. CONCLUSIONS

The results of the  $^{27}\text{Al}$  NMR spectrum and spin-lattice relaxation studies of icosahedral  $\text{Al}_{72.4}\text{Pd}_{20.5}\text{Mn}_{7.1}$  are compatible with the hypothesis that a screening electron cloud is formed around (probably a part of) the Mn ions in an aluminum-rich environment. The electrons produce a large EFG at the sites of the close Al nuclei that is temperature-dependent due to the polarization of the screening and core electrons by the magnetic moments of the Mn unpaired  $d$  electrons. The increase of the EFG on cooling produces an inverse temperature dependence of the width and frequency shift of the  $^{27}\text{Al}$  NMR spectrum. The shift of the  $^{27}\text{Al}$  central line was found to be inversely proportional to the external magnetic field, as characteristic for a second-order electric quadrupolar shift. The  $^{27}\text{Al}$  spin-lattice relaxation rate shows an  $aT + bT^3$  dependence that can be explained by approximating the actual quasicrystalline electronic structure by a two-band model of a regular, structurally periodic metal. The  $T^3$  term originates from the narrowness of the  $d$  conduction band, or more precisely from the fact that the  $d$ -electron density of states cannot be considered as constant over the energy interval  $k_B T$  around  $E_F$ . The appearance of the  $T^3$  term in quasicrystals by itself does not prove the existence of sharp features inside the pseudogap in the DOS at the Fermi level but merely reflects the narrowness of the  $d$  conduction band. The  $^{27}\text{Al}$  spin-lattice relaxation in  $\text{Al}_{72.4}\text{Pd}_{20.5}\text{Mn}_{7.1}$  is governed by two relaxation mechanisms of similar strength, the electric quadrupole and the magnetic hyperfine. The quadrupole mechanism is stronger at high temperatures such as room temperature whereas at temperatures close to that of liquid He the magnetic relaxation becomes dominant. Spin-

lattice relaxation in icosahedral Al-Pd-Mn is thus more complex than assumed so far and cannot be accounted for by a single relaxation process. Though the two-band model reproduces well the observed temperature dependence of the relaxation rates, it fails even qualitatively to reproduce the observed magnetic-field dependence of the rates. A better theory of the spin-lattice relaxation in quasicrystals—unfortunately not existing as yet—should take into account

the proper quasicrystalline electronic structure in the form of critical states instead of extended waves.

#### ACKNOWLEDGMENTS

We are most grateful to Dr. J. M. Dubois from Ecole des Mines de Nancy and to Dr. N. Tamura and Dr. K. Urban from Jülich Research Center for the provision of the sample.

\*On leave from Institute of Physics of Solids and Semiconductors, Minsk, Belarus.

<sup>1</sup>S. J. Poon, *Adv. Phys.* **41**, 303 (1992).

<sup>2</sup>T. Klein, C. Berger, D. Mayou, and F. Cyrot-Lackmann, *Phys. Rev. Lett.* **66**, 2907 (1991).

<sup>3</sup>D. Mayou, C. Berger, F. Cyrot-Lackmann, T. Klein, and P. Lanco, *Phys. Rev. Lett.* **70**, 3915 (1993).

<sup>4</sup>F. S. Pierce, S. J. Poon, and B. D. Biggs, *Phys. Rev. Lett.* **70**, 3919 (1993).

<sup>5</sup>B. D. Biggs, S. J. Poon, and N. R. Munirathnam, *Phys. Rev. Lett.* **65**, 2700 (1990).

<sup>6</sup>F. S. Pierce, Q. Guo, and S. J. Poon, *Phys. Rev. Lett.* **73**, 2220 (1994).

<sup>7</sup>T. Fujiwara and T. Yokokawa, *Phys. Rev. Lett.* **66**, 333 (1991).

<sup>8</sup>A. P. Smith and N. W. Ashcroft, *Phys. Rev. Lett.* **59**, 1365 (1987).

<sup>9</sup>M. Krajčí, M. Windisch, J. Hafner, G. Kresse, and M. Mihalkovič, *Phys. Rev. B* **51**, 17 355 (1995).

<sup>10</sup>X.-P. Tang, E. A. Hill, S. K. Wonnell, S. J. Poon, and Y. Wu, *Phys. Rev. Lett.* **79**, 1070 (1997).

<sup>11</sup>A. Shastri, D. B. Baker, M. S. Conradi, F. Borsa, and D. R. Torgeson, *Phys. Rev. B* **52**, 12 681 (1995).

<sup>12</sup>Z. M. Stadnick, G. W. Zhang, A. P. Tsai, and A. Inoue, *J. Phys.: Condens. Matter* **6**, 6885 (1994).

<sup>13</sup>E. A. Hill, T. C. Chang, Y. Wu, S. J. Poon, F. S. Pierce, and Z. M. Stadnick, *Phys. Rev. B* **49**, 8615 (1994).

<sup>14</sup>J. L. Gavilano, B. Ambrosini, P. Vonlanthen, M. A. Chernikov, and H. R. Ott, *Phys. Rev. Lett.* **79**, 3058 (1997).

<sup>15</sup>A. Shastri, F. Borsa, D. R. Torgeson, J. E. Shield, and A. I. Goldman, *Phys. Rev. B* **50**, 15 651 (1994).

<sup>16</sup>M. A. Chernikov, A. Bernasconi, C. Beeli, A. Schilling, and H. R. Ott, *Phys. Rev. B* **48**, 3058 (1993).

<sup>17</sup>J. C. Lasjaunias, A. Sulpice, N. Keller, J. J. Préjean, and M. de Boissieu, *Phys. Rev. B* **52**, 886 (1995).

<sup>18</sup>J. Friedel, *Can. J. Phys.* **34**, 1190 (1956).

<sup>19</sup>W. Kohn and S. H. Vosko, *Phys. Rev.* **119**, 912 (1960).

<sup>20</sup>A. Blandin and J. Friedel, *J. Phys. Radium* **21**, 689 (1960).

<sup>21</sup>J. M. Brettel and J. Heeger, *Phys. Rev.* **153**, 319 (1967).

<sup>22</sup>A. Narath, *Phys. Rev.* **162**, 320 (1967).

<sup>23</sup>E. R. Andrew and D. P. Tunstall, *Proc. Phys. Soc. (London)* **78**, 1 (1961).

<sup>24</sup>See, C. Janot, *Quasicrystals* (Clarendon, Oxford, 1994), p. 382.

<sup>25</sup>J. Winter, *Magnetic Resonance in Metals* (Clarendon, Oxford, 1971), pp. 115–118.

<sup>26</sup>Y. Obata, *J. Phys. Soc. Jpn.* **19**, 2348 (1964).

<sup>27</sup>C. Janot, A. Magerl, B. Frick, M. de Boissieu, *Phys. Rev. Lett.* **71**, 871 (1993).